

Relative Reactivities of Isobutylene, Styrene, and Ring-Substituted Styrenes in Cationic Polymerizations

Nagesh Kolishetti and Rudolf Faust*

Polymer Science Program, Department of Chemistry, University of Massachusetts Lowell,
One University Avenue, Lowell, Massachusetts 01854

Received January 17, 2008; Revised Manuscript Received March 24, 2008

ABSTRACT: The addition reaction of isobutylene (IB), styrene (St), *p*-methylstyrene (*p*MeSt), and *p*-chlorostyrene (*p*ClSt) to living poly(*p*-methoxystyrene) (PpMeOSt) obtained using the 1-chloro-1-(*p*-methoxyphenyl)ethane/tin tetrabromide (*p*MeOStCl/SnBr₄) initiating system in dichloromethane (CH₂Cl₂) and CH₂Cl₂/methylcyclohexane (MeCHx) from −40 to 0 °C in the presence of 2,6-di-*tert*-butylpyridine (DTBP) as a proton trap was studied. Quantitative crossover to IB, St, *p*MeSt, and *p*ClSt was observed, and changing the temperature, solvent polarity, and concentrations could control the number of capping monomer units incorporated per chain before irreversible ion collapse. Accordingly, the polymerization of *p*MeOSt in the presence of IB, St, *p*MeSt, or *p*ClSt stopped short of completion. These so-called competition experiments were used to determine the reactivity ratios, k_p/k_{12} , where k_p is the propagation rate constant of *p*MeOSt and k_{12} is the cross-propagation rate constant. On the basis of the reactivity ratios calculated from the limiting conversions and limiting molecular weights, in CH₂Cl₂/MeCHx at −40 °C, *p*MeOSt is 42, 271, 291, and 771 times more reactive than *p*MeSt, IB, St, and *p*ClSt, respectively. A similar reactivity order was established with CH₂Cl₂ as solvent at −40 °C. With increasing temperature differences in reactivities decreased. With the published k_p values the cross-propagation rate constants were calculated. A comparison of the k_{12} values and the propagation rate constants of the different monomers reported before indicated that substituents have a much larger effect on the cation reactivity than on the monomer reactivity.

Introduction

Kinetic and mechanistic understanding of a polymerization process is very important from the fundamental point of view.^{1,2} In the past few years we have reported on the utilization of the reaction clock method to determine the rate constant of propagation (k_p) as well as the rate (k_i) and equilibrium constant of ionization (K_i) and deactivation (k_{-i}) in the carbocationic polymerization of IB,³ St,⁴ and ring-substituted styrenes.^{5–8} The reaction clock method references the unknown rate constant for the reaction of the intermediate cation to that for a second reaction with a known rate constant, which serves as a “clock”. In the diffusion clock method the “clock” speed is the diffusion limit.⁹ The results are summarized in Table 1, where the styrenic monomers are arranged in the order of their decreasing k_p .

With increasing electron-donating ability of the substituents on the phenyl ring of styrene, the reactivity of the monomer increases and the reactivity of the corresponding cation decreases. Although electronic factors affect both the monomer and cation reactivity, the separation of these effects is complex, and a general and quantitative treatment has not yet been developed. The results in Table 1 suggest that k_p is mainly determined by the reactivity of the cation since the increase in the reactivity of the monomer is much smaller than the decrease in the reactivity of the cation. The k_p value is lower for *p*-methylstyrene and much lower for *p*-methoxystyrene and 2,4,6-trimethylstyrene compared to that for styrene, which demonstrates that, contrary to previous teachings,¹⁰ these two effects do not cancel each other. With bulky reagents steric effects could also become important. For instance, although k_p is almost identical for *p*-methoxystyrene and 2,4,6-trimethylstyrene, separate studies showed that the nucleophilic reactivity of 2,4,6-trimethylstyrene is similar to styrene¹¹ due to cancelation of the electron donating effect by the distortion of coplanarity between the vinylic double bond and the aromatic ring.

Recently, we have been interested to develop a structure–reactivity relationship for monomers and polymer carbocations. Most of our knowledge on carbocation and alkene reactivity has been based on a general method developed by Mayr, who first recognized the kinetic utility of the fact that under special conditions when the formation of the [1:1] adduct is faster than its consumption, carbocations react with olefins to yield [1:1] adduct exclusively (Scheme 1).¹²

In case A covalent products are formed from ionic reactants (Scheme 1). This case has been exploited by Mayr^{2,12} to determine the nucleophilicity parameter, N , to characterize nucleophilic reactivity of alkenes. In case B ionic products are formed from covalent reactants. This methodology was used for the capping reactions by Faust and co-workers.¹³ We have recently reported on the kinetic utility of case C, where covalent products are formed from the covalent reactants, and employed this method to establish the relative reactivity of C4 olefins against the polyisobutylene (PIB) cation.¹⁴ Under conditions where the reaction of P_1^+ (propagating cation of monomer M_1) with M_2 (terminating monomer M_2) results in the exclusive formation of [1:1] adduct, the cross-propagation rate constant (k_{12}) could be calculated from the reactivity ratio $r_1 = k_p/k_{12}$ using the known value of k_p (propagation rate constant for M_1). The value of r_1 could be easily determined from the limiting conversion (x_∞) or limiting number-average degree of polymerization ($DP_{n\infty}$) from copolymerizations terminating after a single cross-propagation using the equations^{15,16}

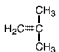
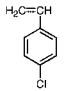
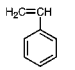
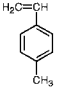
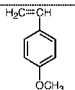
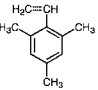
$$\frac{k_p}{k_{12}} = \frac{\ln(1 - x_\infty)}{\ln(1 - [I]_0/[M_2]_0)} \quad (1)$$

$$\frac{k_p}{k_{12}} = \frac{\ln(1 - DP_{n\infty}[I]_0/[M_1]_0)}{\ln(1 - [I]_0/[M_2]_0)} \quad (2)$$

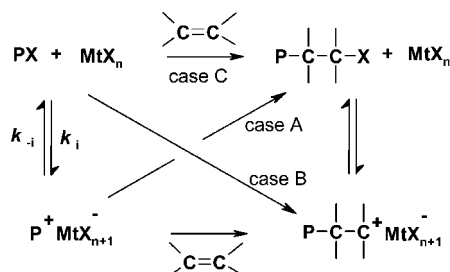
where k_p is the rate constant of propagation for monomer 1 and k_{12} is the cross-propagation rate constant from M_1 to M_2 (Scheme 2). $[I]_0$ is the initial concentration of the initiator, which

* Corresponding author: Tel 1-978-934-3675, Fax 1-978-934-3013.

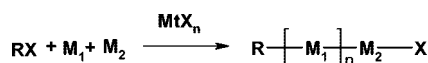
Table 1. Rate and Equilibrium Constants Determined for IB, Styrene, and Ring-Substituted Styrenes

Monomer	Solvent	Lewis Acid (Temp)	k_p^\pm (L mol ⁻¹ s ⁻¹)	K_i^{app} or K_i (L ² mol ⁻² or L mol ⁻¹)	k_i^{app} or k_i (L ² mol ⁻² s ⁻¹ or L mol ⁻¹ s ⁻¹)	k_{-i} (s ⁻¹)	ref
	Hx/MeCl 60/40 (v/v)	TiCl ₄ (-80 °C)	5x10 ⁸	$K_i^{app} = 7.2 \times 10^{-7}$	$k_i^{app} = 16.0$	2.3x10 ⁷	3,16
	MeCHx/MeCl 60/40 (v/v)	TiCl ₄ (-80 °C)	3x10 ⁹	$K_i^{app} = 1.5 \times 10^{-8}$	$k_i^{app} = 0.8$	5.5x10 ⁷	7
	MeCHx/MeCl 60/40 (v/v)	TiCl ₄ (-80 °C)	2x10 ⁹	$K_i^{app} = 1.2 \times 10^{-7}$	$k_i^{app} = 4.0$	3.3x10 ⁷	4
	CH ₂ Cl ₂	SnCl ₄ (-15 °C)	8x10 ⁹				
	MeCHx/MeCl 60/40 (v/v)	TiCl ₄ (-80 °C)	7x10 ⁸				8
	CH ₂ Cl ₂	SnCl ₄ (-60 °C)	1x10 ⁹				
	CH ₂ Cl ₂	TiCl ₄ (-60 °C)	2x10 ⁴	$K_i = 3.1 \times 10^{-2}$			5
	CH ₂ Cl ₂	BCl ₃ (-60 °C)	1.8x10 ⁴	$K_i = 1.4 \times 10^{-3}$	$k_i = 3.0$	2.2x10 ³	6

Scheme 1. Selected Carbocation and Olefin Reaction Pathways



Scheme 2. Schematic Description of Propagation and Cross-Propagation

M₁ - Monomer 1 (*p*MeOSt)M₂ - Monomer 2 (IB, St, *p*MeSt, *p*ClSt)MtX_n - Lewis acid (SnBr₄)

equals that of the chain ends; [M₂]₀ and [M₁]₀ are the initial concentration of monomers. More details regarding the kinetic basis of eqs 1 and 2 are available elsewhere.^{15,16} When k_p is known, k_{i2} can also be calculated, which may be used to develop a quantitative structure–reactivity relationship for both monomers and polymer cations.

The formation of a 1:1 adduct is only feasible under suitable conditions when the reactivity of M₁ is much higher than that of M₂ and further propagation of M₁ or M₂ is not feasible.^{10,13,15} This paper reports on relative reactivities of IB, St, and ring-substituted styrenes toward the *Pp*MeOSt⁺ cation and the calculated cross-propagation rate constants from the poly(*p*-methoxystyryl) cation (*Pp*MeOSt⁺) to IB, St, and ring-substituted styrenes. *Pp*MeOSt⁺ was selected as a reference

electrophile since *p*-methoxystyrene (*p*MeOSt) has the highest nucleophilicity for which the propagation rate constant is known.⁵

Experimental Section

Materials. IB was dried in the gaseous state by passing it through in-line gas-purifier columns packed with BaO/Drierite. It was condensed in the cold bath of a glovebox prior to polymerization. Titanium tetrachloride (TiCl₄, 99.9%), SnBr₄ (99%), and DTBP (97%) were purchased from Aldrich and used as received. The *p*MeOSt (Aldrich, 97%), *p*MeSt (Aldrich, 96%), St (Aldrich, 97%), and *p*ClSt (Aldrich, 99%) were freed from inhibitor by washing with 5% aqueous NaOH solution followed by distilled water until neutral. After drying (or passing) over anhydrous Na₂SO₄, the styrenic monomers were distilled from CaH₂ under reduced pressure and stored under nitrogen at -20 °C, and they were distilled once again from CaH₂ under reduced pressure prior to use. The *p*MeOStCl was synthesized by bubbling dry HCl gas into *p*MeOSt in dry dichloromethane (CH₂Cl₂) (1:10 *p*MeOSt/CH₂Cl₂ (v/v)) under stirring at -78 °C, and then dry nitrogen gas was bubbled for 30 min to remove excess HCl. CH₂Cl₂ was removed using a vacuum pump. Finally, *p*MeOStCl was distilled under vacuum (¹H NMR: 7.41 (d), 6.94 (d), 5.1–5.2 (q), 3.86 (s), and 1.89 (d) ppm). The CH₂Cl₂ was washed with 5% aqueous NaOH solution and then with distilled water until neutral. Then it was predried on anhydrous Na₂SO₄ and distilled from CaH₂ under nitrogen. This distilled CH₂Cl₂ was refluxed under nitrogen overnight with phosphorus pentoxide (P₂O₅) and distilled to a round-bottom flask containing P₂O₅. It was refluxed under nitrogen overnight and distilled just before use. Methylcyclohexane (MeCHx) was refluxed over CaH₂ overnight under nitrogen and distilled before use. Tetrahydrofuran (reagent grade) was refluxed on CaH₂ under a nitrogen atmosphere for 24 h and distilled before use. Methanol (reagent grade) was distilled and used.

Polymerization. Polymerizations were carried out under a dry nitrogen atmosphere in an MBraun 150-M glovebox (Innovative Technology Inc., Newburyport, MA). Large (75 or 150 mL) culture tubes were used as polymerization reactors. The total volume of the reaction mixture was 15 or 45 mL. After predetermined times the

polymerizations were terminated by the addition of 0.5 mL of prechilled methanol. All polymers were purified by reprecipitation from CH_2Cl_2 /methanol twice. Monomer conversions were determined by gravimetric analysis. For chain extension experiments, after the predetermined polymerization time, a fresh charge of monomer was added to the reaction mixture, and the polymerization was continued for a specific time until termination by addition of prechilled methanol.

Capping. In a typical capping experiment into a 150 mL culture tube calculated amounts of CH_2Cl_2 or $\text{CH}_2\text{Cl}_2/\text{MeCHx}$, DTBP stock solution, $p\text{MeOStCl}$ stock solution, and $p\text{MeOSt}$ stock solution were added and mixed thoroughly. The polymerization was started by the addition of SnBr_4 stock solution in CH_2Cl_2 or $\text{CH}_2\text{Cl}_2/\text{MeCHx}$. At the end of polymerization the terminating monomer was added, and after a predetermined time 0.5 mL of prechilled methanol was introduced to quench the polymerization.

Competition. In a typical competition experiment into a 75 mL culture tube calculated amounts of CH_2Cl_2 or $\text{CH}_2\text{Cl}_2/\text{MeCHx}$, DTBP, and $p\text{MeOStCl}$ stock solutions, $p\text{MeOSt}$ and the terminating monomer (IB or St or $p\text{MeSt}$ or $p\text{ClSt}$) were added and mixed thoroughly. The polymerization was started by the addition of SnBr_4 in CH_2Cl_2 or $\text{CH}_2\text{Cl}_2/\text{MeCHx}$. After a predetermined polymerization time 0.5 mL of prechilled methanol was introduced to quench the polymerization.

Characterization. Molecular weights were measured with a Waters GPC system equipped with a model 515 HPLC pump, a model 410 differential refractometer, a Viscostar viscometer (Wyatt Technology Inc.), a model 2847 dual λ absorbance detector, an online multiangle laser light scattering (MALLS) detector (MiniDawn, Wyatt Technology Inc.), a model 712 sample processor, and five Ultrastaygel GPC columns connected in the following series: 500, 10^3 , 10^4 , 10^5 , and 100 \AA . Tetrahydrofuran was used as an eluent at a flow rate of 1.0 mL/min at room temperature. NMR spectroscopy was carried out on a Bruker 500 MHz spectrometer using CDCl_3 as a solvent (Cambridge Isotope Laboratory, Inc.). ^1H NMR spectra of solutions in CDCl_3 were calibrated to tetramethylsilane as internal standard (δ_{H} 0.00). The matrix-assisted laser desorption/ionization (MALDI) time of flight (TOF) mass spectroscopy (MS) measurements were performed with a Waters/Micromass mass spectrometer equipped with a TOF analyzer. The positive ions were detected in reflectron mode. The polymer samples (10 mg/mL) in THF were prepared with a dithranol matrix (20 mg/mL in THF). To produce cations, silver trifluoroacetate (AgTFA) or sodium trifluoroacetate (NaTFA) dissolved in THF at a concentration of 1 mg/mL was added to the matrix/analyte solution. The solutions were mixed in 10:2:1 volume ratio (matrix:analyte:salt). A volume of 0.5 μL of these solutions was deposited onto the target plate (stainless steel) and allowed to air-dry, and the MALDI-TOF-MS spectra were recorded. UV-vis spectroscopic measurements were carried out under a dry nitrogen atmosphere in the glovebox. A quartz immersion probe (661.300-QX, Hellma, optical path 0.5 cm) connected to a fiber-optic visible (tungsten light source, Ocean Optics) and UV (AIS model UV-2, Analytical Instrument Systems, Inc.) light source and a Zeiss MMS 256 photodiode array detector was used. The latter was connected to a personal computer via a TEC5 interface, and the spectra were recorded using the "Aspect Plus" software (Zeiss).

Determination of Rate Constants. The apparent rate constant of propagation (k_{app}) was determined from the slope of $\ln([M]_0/[M])$ vs time plot. The value of K_i was determined from the slope of ionization vs SnBr_4 concentration plot. The value of k_p was calculated from K_i and k_{app} . The reactivity ratios were determined from the x_∞ or from the DP_{n} using eqs 1 and 2.

Results and Discussion

Living Cationic Polymerization of $p\text{MeOSt}$. De and Faust have shown earlier that in conjunction with SnBr_4 as co-initiator and hydrochlorinated p -methoxystyrene ($p\text{MeOStCl}$) as initiator $p\text{MeOSt}$ polymerizes in a living fashion in dichloromethane (CH_2Cl_2) in the temperature range of -60 to -20°C and determined various rate constants.⁵ We have extended these

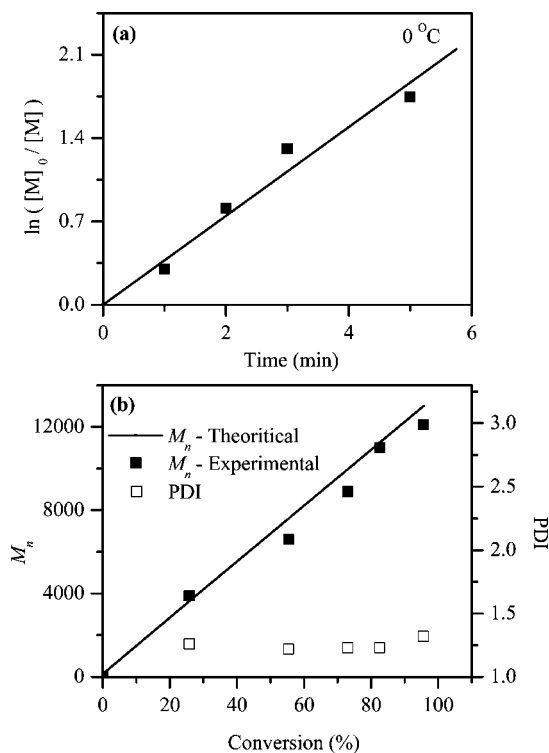


Figure 1. (a) First-order plot of $\ln([M]_0/[M])$ vs time and (b) variation of M_n and PDI with conversion for cationic polymerization of $p\text{MeOSt}$ initiated by $p\text{MeOStCl}/\text{SnBr}_4$ in CH_2Cl_2 at 0°C . [$p\text{MeOSt}$] = 0.2 mol L^{-1} ; [$p\text{MeOStCl}$] = 0.002 mol L^{-1} ; [DTBP] = 0.006 mol L^{-1} ; [SnBr_4] = 0.006 mol L^{-1} .

studies to a $\text{CH}_2\text{Cl}_2/\text{MeCHx}$ (50/50, v/v) solvent mixture and up to 0°C .

Polymerization in CH_2Cl_2 at 0°C . The first-order plot of $\ln([M]_0/[M])$ vs time and variation of M_n with conversion show the expected linearity for living polymerization (Figures 1a,b). The GPC RI traces are shown in Figure S1 in the Supporting Information.

The lifetime of the living centers was studied by chain extension experiments. In these experiments a new feed of $p\text{MeOSt}$ was added to the polymerization mixture after 10 and 15 min and polymerized for an additional 15 min. According to the GPC RI traces shown in Figure 2, decomposition of PpMeOSt^+ is not detected for up to 15 min.

Polymerization in $\text{CH}_2\text{Cl}_2/\text{MeCHx}$ (50/50, v/v). The polymerization of $p\text{MeOSt}$ in $\text{CH}_2\text{Cl}_2/\text{MeCHx}$ (50/50, v/v) was studied at -40 , -20 , and 0°C . The first-order plots are shown in Figure 3a. From the slope of these plots k_{app} was determined to be 4.71×10^{-4} , 5.08×10^{-4} , and $5.52 \times 10^{-4} \text{ s}^{-1}$ for -40 , -20 , and 0°C , respectively. The number-average molecular weight (M_n) and the polydispersity index (PDI) vs conversion plots are shown in Figure 3b.

Using the k_{app} values at different temperatures the apparent activation energy of polymerization, E_a , was calculated to be 2.1 kJ mol^{-1} (Figure S2). It is interesting to note that in CH_2Cl_2 negative E_a (-3.5 kJ mol^{-1}) was obtained.⁵ The reason for this difference is unclear at present.

The linear M_n -conversion plots along with linear first-order plots indicate that the polymerization of $p\text{MeOSt}$ is living in the temperature range of -40 to 0°C . Figures 4, S3, and S4 show the GPC RI traces of the polymers obtained in chain extension studies at -40 , -20 , and 0°C . In these studies a new feed of $p\text{MeOSt}$ was added to the polymerization mixture after 120, 90, and 75 min of polymerization at -40 , -20 , and 0°C , respectively, and the polymerization was continued for

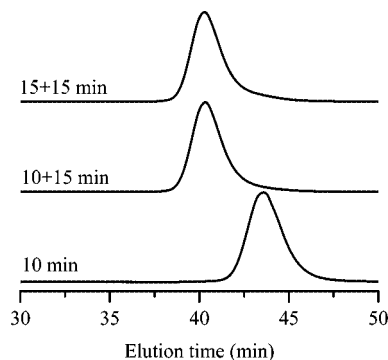


Figure 2. GPC RI traces of poly(*p*MeOSt) from the chain extension experiments of *p*MeOSt⁺ in CH₂Cl₂ at 0 °C. [*p*MeOSt] = 0.03 + 0.06 mol L⁻¹; [*p*MeOStCl] = 0.002 mol L⁻¹; [DTBP] = 0.006 mol L⁻¹; [SnBr₄] = 0.006 mol L⁻¹.

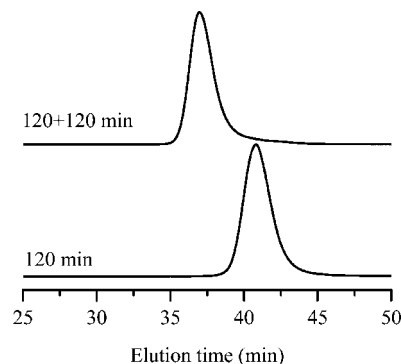


Figure 4. GPC RI traces of poly(*p*MeOSt) from the chain extension experiments of *p*MeOSt⁺ in CH₂Cl₂/MeCHx (50/50, v/v). [*p*MeOSt] = 0.05 + 0.15 mol L⁻¹; [*p*MeOStCl] = 0.001 mol L⁻¹; [DTBP] = 0.006 mol L⁻¹; [SnBr₄] = 0.009 mol L⁻¹; -40 °C.

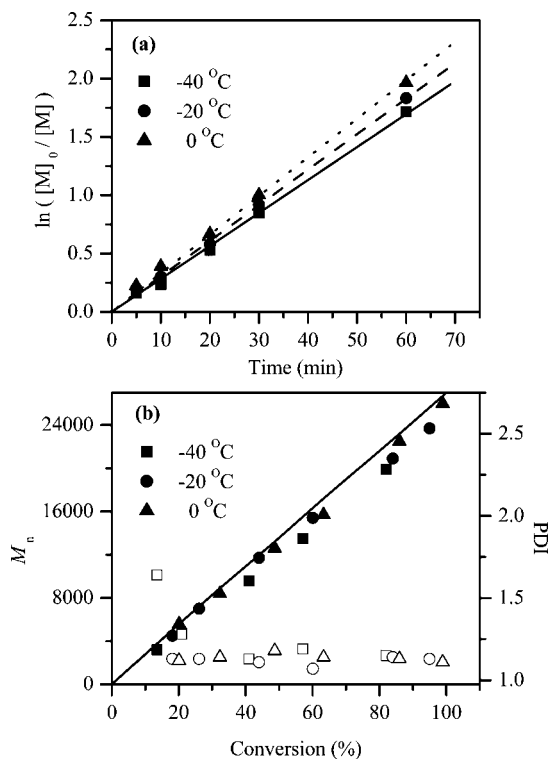


Figure 3. (a) First-order plot of $\ln([M]_0/[M])$ vs time and (b) variation of M_n (filled symbols) and PDI (open symbols) with conversion for cationic polymerization of *p*MeOSt initiated by *p*MeOStCl/SnBr₄ in CH₂Cl₂/MeCHx (50/50, v/v). [*p*MeOSt] = 0.2 mol L⁻¹; [*p*MeOStCl] = 0.001 mol L⁻¹; [DTBP] = 0.006 mol L⁻¹; [SnBr₄] = 0.009 mol L⁻¹.

an additional 120, 90, and 75 min, respectively. In Figures 4, S3, and S4, decomposed *Pp*MeOSt chains cannot be detected. Hence, under these conditions at -40, -20, and 0 °C, the *Pp*MeOSt⁺ is stable for minimum 120, 90, and 75 min, respectively.

Determination of k_p of the Cationic Polymerization of *p*MeOSt Using UV-vis Spectroscopy at -40 °C. To determine the equilibrium constant of ionization, K_i , the ionization of the model compound *p*MeOStCl with SnBr₄ was studied by UV-vis spectroscopy at -40 °C. Ionization of *p*MeOStCl was accomplished by adding *p*MeOStCl to a filtered solution of DTBP and SnBr₄ at -40 °C. The absorbance at 348 nm was used to calculate the percent ionization using the reported^{5,17} molar absorption coefficient $\epsilon_{\max} = 28\,000$ L mol⁻¹ cm⁻¹. The percent ionization is plotted against [SnBr₄] in Figure 5, and

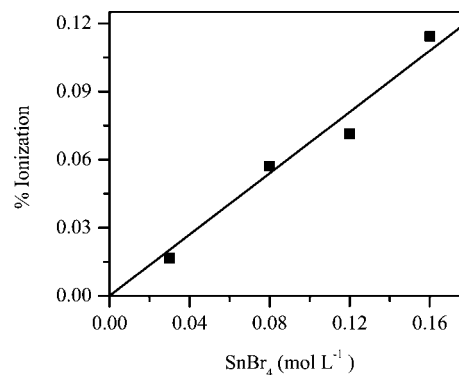


Figure 5. Ionization of *p*MeOStCl by SnBr₄ in CH₂Cl₂/MeCHx (50/50, v/v) at -40 °C. [*p*MeOStCl]₀ = 0.03 mol L⁻¹ and [DTBP] = 0.006 mol L⁻¹.

the straight line shows the linear fit through zero. From the slope of ionization vs SnBr₄ concentration $K_i = 6.7 \times 10^{-3}$ L mol⁻¹ was calculated.

Using $K_i = 6.7 \times 10^{-3}$ L mol⁻¹ and $k_{\text{app}} = 4.71 \times 10^{-4}$ s⁻¹ at -40 °C (Figure 3), $k_p^\pm = 7.8 \times 10^3$ L mol⁻¹ s⁻¹ was calculated. This value is about 8 times lower than the reported k_p^\pm value in CH₂Cl₂ at the same temperature. A similar observation of the effect of solvent polarity on k_p^\pm was reported before.⁴

Capping Reactions of Living *Pp*MeOSt⁺ with IB. The crossover (capping) from living poly(*p*MeOSt) cation to IB was studied at different temperatures and solvent polarities. These capping reactions were carried out at similar conditions to the competition experiments (see later) to ascertain monoaddition of IB to living *Pp*MeOSt, which would be difficult to verify by the analysis of the products of competition experiments due to the high molecular weights. First *p*MeOSt was polymerized in CH₂Cl₂ at -40 °C using [*p*MeOSt] = 0.04 mol L⁻¹, [*p*MeOStCl] = 0.002 mol L⁻¹, [DTBP] = 0.006 mol L⁻¹, and [SnBr₄] = 0.006 mol L⁻¹ for 30 min to achieve quantitative conversion. Then one polymerization tube was quenched with prechilled methanol while to another one IB ([IB] = 0.5 M) was added, and after an additional 30 min the reaction was quenched with prechilled methanol. It has been previously determined that under monomer-starved conditions the polymeric chain ends are stable up to 30 min in CH₂Cl₂ even at -30 °C.⁵ The molecular weights determined by GPC were in good agreement with the theoretical molecular weight assuming that one polymer chain is formed from one molecule of initiator. The capped *Pp*MeOSt-IB-Br and uncapped *Pp*MeOSt-OMe exhibited GPC RI traces (Figure S5) virtually identical in shape and retention time. Quantitative crossover reaction from living *Pp*MeOSt chain

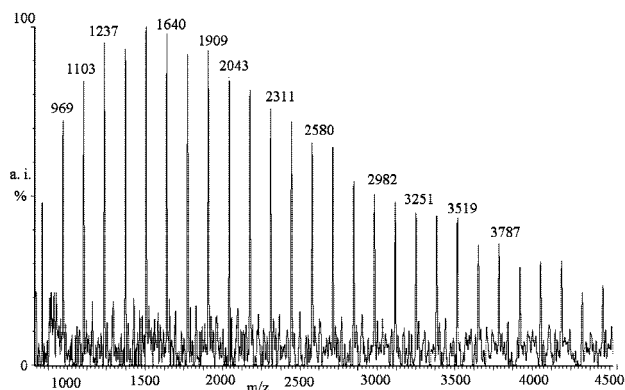


Figure 6. MALDI-TOF MS spectrum of PMeOST-IB-Br prepared using $[p\text{MeOST}] = 0.001 \text{ mol L}^{-1}$, $[\text{DTBP}] = 0.006 \text{ mol L}^{-1}$, $[\text{SnBr}_4] = 0.009 \text{ mol L}^{-1}$, and $\text{CH}_2\text{Cl}_2/\text{MeCHx}$ (50/50, v/v).

end to IB was indicated by the disappearance of the $-\text{OMe}$ chain end at $\sim 3 \text{ ppm}$ in the ^1H NMR spectrum, which is observed when the living polymerization of $p\text{MeOST}$ is quenched with methanol.⁵ Detection of the chain end IB signals in the ^1H NMR spectrum (Figure S6) is not possible as they overlap with that of the polymer backbone. To determine the number of IB units per chain, the capped polymers were analyzed by MALDI-TOF MS studies. A representative spectrum is shown in Figure 6. In agreement with previous reports,¹⁸ HBr elimination under MALDI-TOF MS conditions yields the olefin chain end. The separation between the peaks (134 amu) corresponds to the $p\text{MeOST}$ repeat unit molecular weight, and calculation of the residual mass by subtraction of one unit of silver and multiples of repeat unit molecular weight gave a residue of 56, which corresponds to one IB unit per polymer chain. The very small second series corresponds to PpMeOST chains that added two IB units most likely due to the locally high concentration of IB during the addition of IB.

Capping studies with IB were also carried out at -20 and 0°C in CH_2Cl_2 . At these higher temperatures 10 min polymerization (complete conversion) was followed by capping for 20 min. Further capping studies with IB were carried out in $\text{CH}_2\text{Cl}_2/\text{MeCHx}$ (50/50, v/v) at -40 , -20 , and 0°C using slightly different conditions ($[p\text{MeOST}] = 0.025 \text{ mol L}^{-1}$, $[p\text{MeOSTCl}] = 0.001 \text{ mol L}^{-1}$, $[\text{DTBP}] = 0.006 \text{ mol L}^{-1}$, $[\text{SnBr}_4] = 0.009 \text{ mol L}^{-1}$, and $[\text{IB}] = 0.25 \text{ mol L}^{-1}$). The monomer $p\text{MeOST}$ was polymerized for 120 min followed by the addition of IB and capping reaction for 120 min. In all cases monoaddition of IB was observed from MALDI-TOF MS studies.

Competition Experiments of $p\text{MeOST}$ with IB. Competition experiments, i.e., polymerization of $p\text{MeOST}$ in the presence of the terminating monomer IB, were carried out to determine the reactivity ratios using eqs 1 and 2 and k_{12} using the known value of k_p . Typical time vs conversion plots for the competition experiments of $p\text{MeOST}$ in the presence of IB at -40°C are shown in Figure 7. The conversion (as well as number-average molecular weight, M_n) reached a limiting value in 30 min. The M_n of the polymer, determined by GPC, was in reasonable agreement with the calculated one based on the conversion by assuming that one polymer chain is formed from one molecule of initiator (Table S1). The polydispersity of the polymers were in the range of 1.3–2.1. ^1H NMR spectra of these polymers showed the absence of methoxy chain end protons at $\sim 3 \text{ ppm}$, indicating complete capping by IB. The limiting conversions, molecular weights, and k_p/k_{12} values calculated from x_∞ using eq 1 and from $\text{DP}_{n\infty}$ using eq 2 are listed in Table 2.

According to Table 2, $p\text{MeOST}$ is approximately 200, 171, and 123 times more reactive than IB at -40 , -20 , and 0°C ,

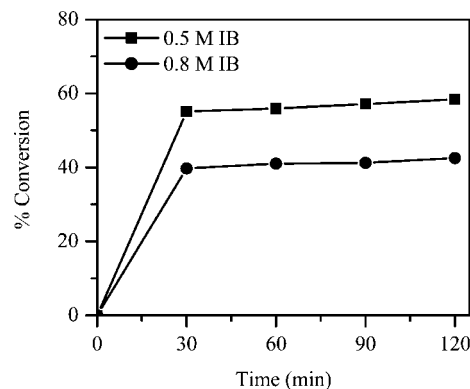


Figure 7. Time vs conversion plots from the competition experiments between $p\text{MeOST}$ and IB in CH_2Cl_2 at -40°C . $[p\text{MeOST}] = 0.2 \text{ mol L}^{-1}$; $[p\text{MeOSTCl}] = 0.002 \text{ mol L}^{-1}$; $[\text{DTBP}] = 0.006 \text{ mol L}^{-1}$; $[\text{SnBr}_4] = 0.006 \text{ mol L}^{-1}$; $[\text{IB}] = 0.5$ and 0.8 mol L^{-1} .

Table 2. Limiting Conversion, Molecular Weight, and k_p/k_{12} Values in the Competition Reactions between $p\text{MeOST}$ and IB in CH_2Cl_2 at Different Temperatures^a

IB (mol L ⁻¹)	temp (°C)	conv (%)	M_n (GPC)	PDI	k_p/k_{12} (conv)	k_p/k_{12} (DP _{n∞})	k_p/k_{12} (av)
0.5	-40	55.1	7500	1.74	200	205	202
0.8	-40	39.7	5200	1.75	202	196	198
0.5	-20	49.7	6600	1.59	172	169	171
0.8	-20	35.0	4700	1.75	172	172	172
0.5	0	38.5	5000	1.89	121	117	119
0.8	0	27.8	3600	1.86	130	125	127

^a $[p\text{MeOST}] = 0.2 \text{ mol L}^{-1}$; $[p\text{MeOSTCl}] = 0.002 \text{ mol L}^{-1}$; $[\text{DTBP}] = 0.006 \text{ mol L}^{-1}$; $[\text{SnBr}_4] = 0.006 \text{ mol L}^{-1}$, time = 30 min.

respectively. According to the Arrhenius plot (see Figure S7 in Supporting Information) constructed using the average reactivity ratios obtained at three different temperatures, the activation energy difference is 6.4 kJ mol^{-1} . The decreasing reactivity ratio with increasing temperature suggests that the activation energy for the addition of IB to PpMeOST^+ (E_{12}) is higher than the corresponding value for the addition of $p\text{MeOST}$ (E_p). Thus, considering the previously reported $E_p = 24.9 \text{ kJ mol}^{-1}$, $E_{12} = 31.3 \text{ kJ mol}^{-1}$.

Competition experiments were also carried out in $\text{CH}_2\text{Cl}_2/\text{MeCHx}$ (50/50, v/v) at -40 , -20 , and 0°C . Figure S9 shows the time vs conversion plots at -40°C . Similar studies were carried at -20 and 0°C (see Tables S5 and S6 in Supporting Information). At all temperatures limiting conversion is reached in $\sim 120 \text{ min}$. The limiting conversions, molecular weights, and k_p/k_{12} values calculated are presented in Table 3. Similar to the results with CH_2Cl_2 , the reactivity ratio decreases with increasing temperature.

From the Arrhenius plot (Figure S9 in Supporting Information) constructed using the average reactivity ratios obtained at three different temperatures, the activation energy for the addition of IB to PpMeOST^+ is 6.1 kJ mol^{-1} higher than the activation energy for the addition of $p\text{MeOST}$ to PpMeOST^+ . This value is similar to that obtained with CH_2Cl_2 .

Capping Reactions of Living PpMeOST^+ with St. The capping of PpMeOST^+ cation with St was carried out in CH_2Cl_2 and in $\text{CH}_2\text{Cl}_2/\text{MeCHx}$ (50/50, v/v) at -40 , -20 , and 0°C . In CH_2Cl_2 $p\text{MeOST}$ was polymerized for 30 min at $[p\text{MeOST}] = 0.04 \text{ mol L}^{-1}$, $[p\text{MeOSTCl}] = 0.002 \text{ mol L}^{-1}$, $[\text{DTBP}] = 0.006 \text{ mol L}^{-1}$, and $[\text{SnBr}_4] = 0.006 \text{ mol L}^{-1}$, and then the capping monomer $[\text{St}] = 0.7 \text{ mol L}^{-1}$ was added; after 30 min the reaction was quenched with prechilled methanol. The molecular weights obtained from GPC measurements were in good agreement with the theoretical molecular weight. The GPC RI traces (Figure S10) of the capped and uncapped polymers were

Table 3. Limiting Conversion, Molecular Weight, and k_p/k_{12} Values in the Competition Reactions between $p\text{MeOSt}$ and IB in $\text{CH}_2\text{Cl}_2/\text{MeCHx}$ (50/50, v/v) at Different Temperatures^a

IB (mol L ⁻¹)	temp (°C)	conv (%)	M_n (GPC)	PDI	k_p/k_{12} (conv)	k_p/k_{12} (DP_{theo})	k_p/k_{12} (av)
0.25	-40	66.5	17 500	1.50	273	278	275
0.4	-40	49.2	12 900	1.78	271	262	267
0.25	-20	57.9	15 200	1.61	216	209	212
0.4	-20	42.0	11 300	1.80	218	219	219
0.25	0	48.4	13 000	1.76	165	166	165
0.4	0	35.8	9 300	2.01	177	170	174

^a $[p\text{MeOSt}] = 0.2 \text{ mol L}^{-1}$; $[p\text{MeOStCl}] = 0.001 \text{ mol L}^{-1}$; $[\text{DTBP}] = 0.006 \text{ mol L}^{-1}$; $[\text{SnBr}_4] = 0.009 \text{ mol L}^{-1}$, time = 120 min.

Table 4. Experimental Results for the Capping Reaction of $Pp\text{MeOSt}^+$ with St in CH_2Cl_2 ^a

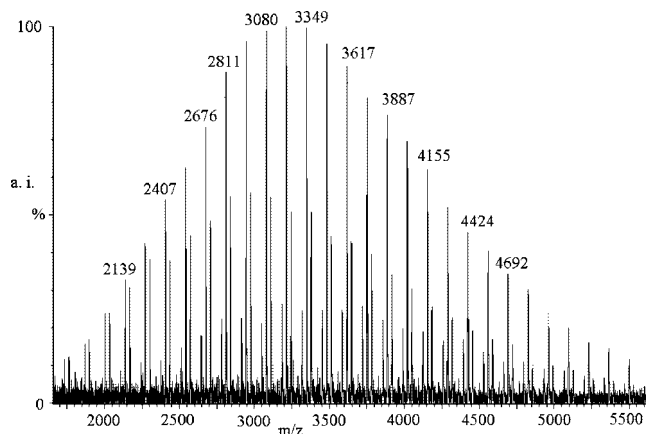
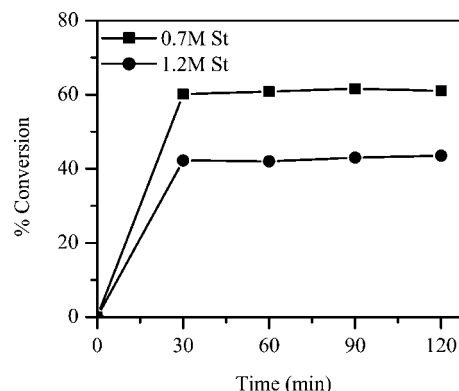
St (mol L ⁻¹)	temp (°C)	time (min)	M_n (GPC)	PDI	no. of St per chain
0.7	-40	30 + 30	2500	1.1	4
0.7	-20	10 + 20	2500	1.1	2.5
0.7	0	10 + 20	2500	1.1	1.5
0.35 ^b	-40	120 + 120	3600	1.1	1.5
0.35 ^b	-20	90 + 90	3600	1.1	1.2
0.35 ^b	0	75 + 75	3600	1.1	1.05

^a Quantitative conversions were obtained with respect to $p\text{MeOSt}$. $[\text{DTBP}] = 0.006 \text{ mol L}^{-1}$, $[p\text{MeOStCl}] = 0.002 \text{ mol L}^{-1}$, $[\text{SnBr}_4] = 0.006 \text{ mol L}^{-1}$. ^b $[p\text{MeOStCl}] = 0.001 \text{ mol L}^{-1}$; $[\text{DTBP}] = 0.006 \text{ mol L}^{-1}$; $[\text{SnBr}_4] = 0.009 \text{ mol L}^{-1}$; $\text{CH}_2\text{Cl}_2/\text{MeCHx}$ (50/50, v/v).

similar in shape and retention time. Quantitative crossover reaction from living $Pp\text{MeOSt}$ chain end to a second monomer was indicated by disappearance of $-\text{OMe}$ chain ends at 3 ppm in the ^1H NMR spectra. Comparison of the aromatic signals of the styrene end units at 7–7.2 ppm to that of methyl headgroup from the initiator at 1 ppm in the ^1H NMR spectra (Figure S11) shows that the number of incorporated styrene units per chain decreases from 4 at -40°C to 1.5 at 0°C (Table 4) due to the increase of the rate constant of ion collapse with increasing temperature.⁶

Capping studies with St in $\text{CH}_2\text{Cl}_2/\text{MeCHx}$ (50/50, v/v) were carried out under slightly modified conditions ($[p\text{MeOSt}] = 0.025 \text{ mol L}^{-1}$, $[p\text{MeOStCl}] = 0.001 \text{ mol L}^{-1}$, $[\text{DTBP}] = 0.006 \text{ mol L}^{-1}$, $[\text{SnBr}_4] = 0.009 \text{ mol L}^{-1}$, and $[\text{St}] = 0.35 \text{ mol L}^{-1}$). For the capping studies in this reduced polarity medium, 120 min of polymerization was followed by 120 min of capping. ^1H NMR and MALDI-TOF MS studies were performed to characterize the polymers. The results are also included in Table 4. A representative MALDI-TOF MS figure of St-capped $Pp\text{MeOSt}$ is shown in Figure 8. Generally the decrease of solvent polarity increases the rate constant of ion collapse; this results in a decreased number of St units incorporated. In $\text{CH}_2\text{Cl}_2/\text{MeCHx}$ (50/50, v/v) in the studied temperature range all products showed MALDI-TOF spectra where the main peak corresponded to $Pp\text{MeOSt}$ capped with one unit of St with an olefin end due to the elimination of HBr. From Figure 8 the separation between the peaks (134 amu) corresponds to the repeat unit, $p\text{MeOSt}$ molecular weight, and calculation of residual mass by subtraction one unit of sodium and multiple repeat units gave a residue of 104 amu, which corresponds to one St unit per polymer chain. The other two series of small peaks gave a residue of 208 and 0 amu, corresponding to 2 and 0 St units per chain. The absence of St is possibly due to a loss of St during the analysis.

Competition Experiments of $p\text{MeOSt}$ with St. The time vs conversion plots for the competition experiments of $p\text{MeOSt}$ in the presence of St at -40°C are shown in Figure 9. The conversion as well as the number-average molecular weight reached a limiting value in 30 min for all other temperatures (see Tables S7–S9 in Supporting Information). The M_n of the polymer, determined by GPC, was in reasonable agreement with

**Figure 8.** MALDI-TOF mass spectrum of the product obtained in the capping of living $Pp\text{MeOSt}^+$ with St in $\text{CH}_2\text{Cl}_2/\text{MeCHx}$ (50/50, v/v) at -40°C .**Figure 9.** Time vs conversion plots from the competition experiments between $p\text{MeOSt}$ and St in CH_2Cl_2 at -40°C . $[p\text{MeOSt}] = 0.2 \text{ mol L}^{-1}$; $[p\text{MeOStCl}] = 0.002 \text{ mol L}^{-1}$; $[\text{DTBP}] = 0.006 \text{ mol L}^{-1}$; $[\text{SnBr}_4] = 0.006 \text{ mol L}^{-1}$; $[\text{St}] = 0.7$ and 1.2 mol L^{-1} .

the theoretical one based on the conversion by assuming that one polymer chain is formed from one molecule of initiator. The polydispersity index of the polymers was in the range of 1.3–2.1. ^1H NMR studies of these polymers showed the absence of methoxy chain end protons at $\sim 3 \text{ ppm}$ due to complete capping.

The limiting conversions, molecular weights, and calculated k_p/k_{12} values are tabulated in Table 5. According to the capping studies, multiple addition of St is likely, especially in CH_2Cl_2 at low temperature. However, this does not affect the kinetic evaluation since these are most likely St diads, triads, etc., at the end of the polymer chain and not isolated St units. When cross-propagation takes place and the $Pp\text{MeOSt-St}^+$ cation is formed, even if it does not terminate instantaneously it is much more likely to add St than $p\text{MeOSt}$ since both are diffusion limited and $[\text{St}] \gg [p\text{MeOSt}]$. According to the results in Table 5, $p\text{MeOSt}$ is ~ 340 , 245 , and 200 times more reactive than St at -40 , -20 , and 0°C , respectively. As observed for IB, the reactivity ratio decreases with the increase of temperature due to the larger activation energy for cross-propagation compared to propagation. From the Arrhenius plot (Figure S12 in Supporting Information) this difference is 6.4 kJ mol^{-1} , identical with the value obtained with IB.

Figure S13 shows the time vs conversion plots from the competition experiments for $\text{CH}_2\text{Cl}_2/\text{MeCHx}$ (50/50, v/v) at -40°C . (See Tables S11 and S12 in Supporting Information for the results at -20 and 0°C .) The limiting conversions, molecular weights, and k_p/k_{12} values are shown in Table 6. Similarly to the results in CH_2Cl_2 with the increase of temperature the

Table 5. Limiting Conversion, Molecular Weight, and k_p/k_{12} Values in the Competition Reactions between $p\text{MeOSt}$ and St in CH_2Cl_2 at Different Temperatures^a

St (mol L ⁻¹)	temp (°C)	conv (%)	M_n (GPC)	PDI	k_p/k_{12} (conv)	k_p/k_{12} ($\text{DP}_{n\infty}$)	k_p/k_{12} (av)
0.7	-40	60.1	8100	1.5	321	324	322
1.2	-40	42.2	6500	2.1	329	397	363
0.7	-20	47.9	7200	1.7	228	268	248
1.2	-20	30.1	4900	1.8	214	272	243
0.7	0	40.0	6300	1.6	178	221	199
1.2	0	25.1	4300	1.5	172	231	201

^a $[p\text{MeOSt}] = 0.2 \text{ mol L}^{-1}$; $[p\text{MeOStCl}] = 0.002 \text{ mol L}^{-1}$; $[\text{DTBP}] = 0.006 \text{ mol L}^{-1}$; $[\text{SnBr}_4] = 0.006 \text{ mol L}^{-1}$, time = 30 min.

Table 6. Limiting Conversion, Molecular Weight, and k_p/k_{12} Values in the Competition Reactions between $p\text{MeOSt}$ and St in $\text{CH}_2\text{Cl}_2/\text{MeCHx}$ (50/50, v/v) at Different Temperatures^a

St (mol L ⁻¹)	temp (°C)	conv (%)	M_n (GPC)	PDI	k_p/k_{12} (conv)	k_p/k_{12} ($\text{DP}_{n\infty}$)	k_p/k_{12} (av)
0.35	-40	55.6	13 800	1.65	284	252	268
0.6	-40	40.7	11 500	1.56	313	316	314
0.35	-20	53.4	13 900	1.67	266	255	260
0.6	-20	35.8	9 500	1.78	267	262	264
0.35	0	43.3	11 100	1.72	198	186	192
0.6	0	29.1	7 800	1.66	206	205	205

^a $[p\text{MeOSt}] = 0.2 \text{ mol L}^{-1}$; $[p\text{MeOStCl}] = 0.001 \text{ mol L}^{-1}$; $[\text{DTBP}] = 0.006 \text{ mol L}^{-1}$; $[\text{SnBr}_4] = 0.009 \text{ mol L}^{-1}$, time = 120 min.

reactivity ratio decreases. From the experimental results at two different solvent polarities, the reactivity ratio decreases slightly with the decrease of solvent polarity; similar observations with temperature and solvent polarity were seen in earlier studies.¹⁴

From the Arrhenius plot (Figure S14 in Supporting Information) of the average reactivity ratios, $E_p - E_{12} = -5.2 \text{ kJ mol}^{-1}$.

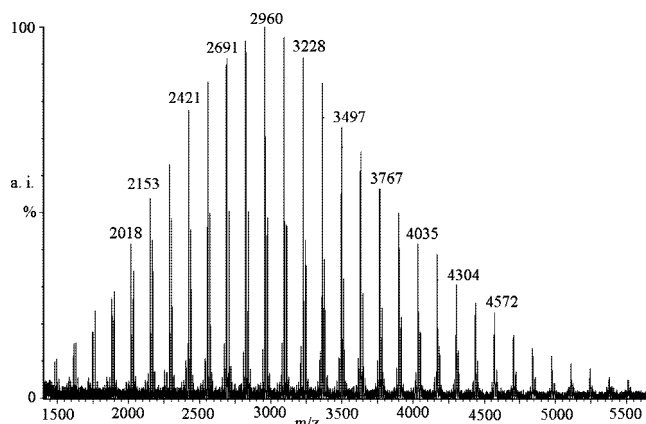
Capping Reactions of Living $p\text{PpMeOSt}^+$ with $p\text{MeSt}$. The results of capping studies with $p\text{MeSt}$ carried out in CH_2Cl_2 at -40, -20, and 0 °C are shown in Table 7. The molecular weights obtained from GPC were in good agreement with the theoretical molecular weight. The M_n s and PDIs of the capped and uncapped polymers were very similar. Quantitative cross-over reaction from living $p\text{PpMeOSt}$ chain end to a second monomer was confirmed from ¹H NMR and MALDI-TOF studies. The ¹H NMR spectra (Figure S15) showed the presence of small amount (<5% of chain ends) of -OMe chain ends. From the MALDI-TOF studies these are $-p\text{MeSt-OMe}$ chain ends possibly due to nucleophilic displacement of bromide end groups with -OMe groups. Comparison of the methyl units of $p\text{MeSt}$ signals to that of methyl headgroup from the initiator at 1 ppm from ¹H NMR spectra show 3, 1.4, and 1.2 units of $p\text{MeSt}$ per chain at -40, -20, and 0 °C.

Further capping studies with $p\text{MeSt}$ were carried out in $\text{CH}_2\text{Cl}_2/\text{MeCHx}$ (50/50, v/v) using slightly modified conditions: $[p\text{MeOSt}] = 0.025 \text{ mol L}^{-1}$; $[p\text{MeOStCl}] = 0.001 \text{ mol L}^{-1}$; $[\text{DTBP}] = 0.006 \text{ mol L}^{-1}$; $[\text{SnBr}_4] = 0.009 \text{ mol L}^{-1}$, and $[p\text{MeSt}] = 0.05 \text{ mol L}^{-1}$. For the capping studies in this reduced polarity medium, 120 min of polymerization followed by 120 min of capping was carried out at -40 °C. ¹H NMR and MALDI-TOF MS studies were performed to characterize all the polymers. A representative MALDI TOF MS of $p\text{MeSt}$ -capped $p\text{PpMeOSt}$ is shown in Figure 10. The separation between the peaks (134 amu) corresponds to the repeat unit, $p\text{MeOSt}$, molecular weight, and calculation of residual mass by subtraction of one unit of sodium and multiple of repeat unit molecular weight gave a residue of 118, which corresponds to one $p\text{MeSt}$ unit per polymer chain. Under MALDI-TOF MS experimental conditions HBr elimination is observed. The other series of small peaks give residues of 236, 0, and 151 after subtraction of repeat unit molecular weight, which correspond to two or 0 $p\text{MeSt}$ units per chain and the 151 residue corresponds to the

Table 7. Experimental Results for the Capping Reaction of $p\text{PpMeOSt}^+$ with $p\text{MeSt}$ in CH_2Cl_2 ^a

$p\text{MeSt}$ (mol L ⁻¹)	temp (°C)	time (min)	M_n (GPC)	PDI	no. of $p\text{MeSt}$ per chain
0.1	-40	30 + 30	2500	1.1	3
0.1	-20	10 + 20	2500	1.2	1.4
0.1	0	10 + 20	2500	1.2	1.2
0.05 ^b	-40	120 + 120	3500	1.1	1.5
0.05 ^b	-20	90 + 90	3500	1.1	1.1
0.05 ^b	0	75 + 75	3500	1.1	1.05

^a Quantitative conversions were obtained with respect to $p\text{MeOSt}$. $[\text{DTBP}] = 0.006 \text{ mol L}^{-1}$, $[p\text{MeOStCl}] = 0.002 \text{ mol L}^{-1}$, $[\text{SnBr}_4] = 0.006 \text{ mol L}^{-1}$. ^b $[p\text{MeOStCl}] = 0.001 \text{ mol L}^{-1}$; $[\text{DTBP}] = 0.006 \text{ mol L}^{-1}$; $[\text{SnBr}_4] = 0.009 \text{ mol L}^{-1}$; $\text{CH}_2\text{Cl}_2/\text{MeCHx}$ (50/50, v/v).

**Figure 10.** MALDI-TOF spectrum of $p\text{OMESt-MeSt-Br}$ prepared using $[p\text{MeOStCl}] = 0.001 \text{ mol L}^{-1}$, $[\text{DTBP}] = 0.006 \text{ mol L}^{-1}$, $[\text{SnBr}_4] = 0.009 \text{ mol L}^{-1}$, and $\text{CH}_2\text{Cl}_2/\text{MeCHx}$ (50/50, v/v) at -40 °C.

$p\text{PpMeOSt-pMeSt-OMe}$.

Competition Experiments of $p\text{MeOSt}$ with $p\text{MeSt}$. The time vs conversion plots for the competition experiments of $p\text{MeOSt}$ in the presence of $p\text{MeSt}$ at -40 °C are shown in Figure 11. The conversion as well as the number-average molecular weight reached a limiting value in 30 min. The M_n of the polymer, determined by GPC, was in reasonable agreement with the theoretical molecular weight. The polydispersity index of the polymers was in the range of 1.3–2.1. The small amount (<5% of chain ends) of methoxy groups observed in the ¹H NMR spectra are due to nucleophilic displacement of bromo end groups in $p\text{PpMeOSt-pMeSt-Br}$ by methanol.

Table 8 gives the reactivity ratios obtained from the competition studies with $p\text{MeSt}$ at -40, -20, and 0 °C. From the average reactivity ratios $p\text{MeOSt}$ is 42, 36, and 30 times more reactive than $p\text{MeSt}$ at -40, -20, and 0 °C, respectively. Similar to earlier observations, the reactivity ratio decreases with the increase of temperature due to different activation energies for propagation and cross-propagation ($E_p - E_{12} = -4.0 \text{ kJ mol}^{-1}$; see Figure S17 in Supporting Information). As expected from the smaller reactivity difference of the two monomers, $E_p - E_{12}$ is smaller than that determined with St or IB .

Competition studies with $p\text{MeSt}$ were also carried out in $\text{CH}_2\text{Cl}_2/\text{MeCHx}$, (50/50, v/v). Figure S18 shows the time vs conversion plots for -40 °C. (For the time vs conversion plots for -20 and 0 °C see Tables S17 and S18 in Supporting Information). The limiting conversions (reached in 120 min), molecular weights, and k_p/k_{12} values are presented in Table 9.

From the Arrhenius plot (Figure S19 in Supporting Information) $E - E_{12} = -5.4 \text{ kJ mol}^{-1}$. The average reactivity ratios are slightly lower than the corresponding values obtained for CH_2Cl_2 , and they show the same trend as a function of temperature.

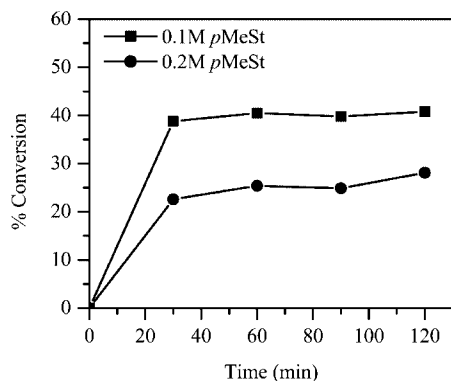


Figure 11. Time vs conversion plots from the competition experiments between *p*MeOSt and *p*MeSt in CH_2Cl_2 at $-40\text{ }^\circ\text{C}$. [*p*MeOSt] = 0.2 mol L^{-1} ; [*p*MeOStCl] = 0.002 mol L^{-1} ; [DTBP] = 0.006 mol L^{-1} ; [*SnBr}_4*] = 0.006 mol L^{-1} ; [*p*MeSt] = 0.1 and 0.2 mol L^{-1} .

Table 8. Limiting Conversion, Molecular Weight, and k_p/k_{12} Values in the Competition Reactions between *p*MeOSt and *p*MeSt in CH_2Cl_2 at Different Temperatures^a

<i>p</i> MeSt (mol L^{-1})	temp ($^\circ\text{C}$)	conv (%)	M_n (GPC)	PDI	k_p/k_{12} (conv)	k_p/k_{12} (DP_{∞})	k_p/k_{12} (av)
0.1	-40	44.7	8300	1.5	29	48	38
0.2	-40	29.6	5800	1.5	35	56	45
0.1	-20	47.7	7300	1.7	32	40	36
0.2	-20	28.1	4500	1.9	33	41	37
0.1	0	40.7	6200	2.0	26	31	28
0.2	0	24.3	4300	2.0	28	38	32

^a [*p*MeOSt] = 0.2 mol L^{-1} ; [*p*MeOStCl] = 0.002 mol L^{-1} ; [DTBP] = 0.006 mol L^{-1} ; [*SnBr}_4*] = 0.006 mol L^{-1} , time = 30 min.

Table 9. Limiting Conversion, Molecular Weight, and k_p/k_{12} Values in the Competition Reactions between *p*MeOSt and *p*MeSt in $\text{CH}_2\text{Cl}_2/\text{MeCHx}$ (50/50, v/v) at Different Temperatures^a

<i>p</i> MeSt (mol L^{-1})	temp ($^\circ\text{C}$)	conv (%)	M_n (GPC)	PDI	k_p/k_{12} (conv)	k_p/k_{12} (DP_{∞})	k_p/k_{12} (av)
0.05	-40	52.2	15 200	1.66	36	41	38
0.1	-40	33.5	11 000	1.75	40	52	46
0.05	-20	45.2	12 800	1.76	30	32	31
0.1	-20	29.6	8 600	1.72	35	38	36
0.05	0	39.7	10 700	1.75	25	25	25
0.1	0	26.1	7 700	1.69	30	33	31

^a [*p*MeOSt] = 0.2 mol L^{-1} ; [*p*MeOStCl] = 0.001 mol L^{-1} ; [DTBP] = 0.006 mol L^{-1} ; [*SnBr}_4*] = 0.009 mol L^{-1} , time = 120 min.

Capping Reactions of Living *Pp*MeOSt⁺ with *p*ClSt. Table 10 shows the results of capping studies with *p*ClSt at various temperatures. Quantitative crossover reaction from living *Pp*MeOSt⁺ to *p*ClSt was indicated in the ^1H NMR spectrum by the disappearance of $-\text{OMe}$ chain ends at $\sim 3\text{ ppm}$ (Figure S20). On the basis of the ratio of aromatic protons of *p*ClSt at 7–7.25 ppm to that of methyl protons of the headgroup at 1 ppm 1.1, 1.0, and 1.0 units of *p*ClSt per chain were calculated for -40 , -20 and $0\text{ }^\circ\text{C}$, respectively.

^1H NMR and MALDI-TOF MS studies were performed to characterize all polymers. These results essentially indicate monoaddition of *p*ClSt at all temperatures and solvent polarity investigated. A representative MALDI-TOF MS figure of *p*ClSt-capped *Pp*MeOSt is shown in Figure 12. The separation between the peaks (134 amu) corresponds to the repeat unit *p*MeOSt molecular weight, and calculation of the residual mass by subtraction of the mass of sodium and multiple repeat units gave a residue of 138 amu, which corresponds to one *p*ClSt unit per polymer chain. Similar to previous observation HBr elimination is observed under MALDI conditions.

Competition Experiments of *p*MeOSt with *p*ClSt. The time vs conversion plots for the competition experiments of *p*MeOSt

Table 10. Experimental Results for the Capping Reaction of *Pp*MeOSt⁺ with *p*ClSt in CH_2Cl_2 ^a

<i>p</i> ClSt (mol L^{-1})	temp ($^\circ\text{C}$)	time (min)	M_n (GPC)	PDI	no. of <i>p</i> ClSt per chain
1.0	-40	30 + 30	2500	1.1	1.1
1.0	-20	10 + 20	2500	1.2	1.0
1.0	0	10 + 20	2500	1.2	1.0
0.5^b	-40	120 + 120	3500	1.1	1.0
0.5^b	-20	90 + 90	3500	1.1	1.0
0.5^b	0	75 + 75	3500	1.1	1.0

^a Quantitative conversions were obtained with respect to *p*MeOSt. [DTBP] = 0.006 mol L^{-1} , [*p*MeOStCl] = 0.002 mol L^{-1} , [*SnBr}_4*] = 0.006 mol L^{-1} . ^b [*p*MeOStCl] = 0.001 mol L^{-1} ; [DTBP] = 0.006 mol L^{-1} ; [*SnBr}_4*] = 0.009 mol L^{-1} ; $\text{CH}_2\text{Cl}_2/\text{MeCHx}$ (50/50, v/v).

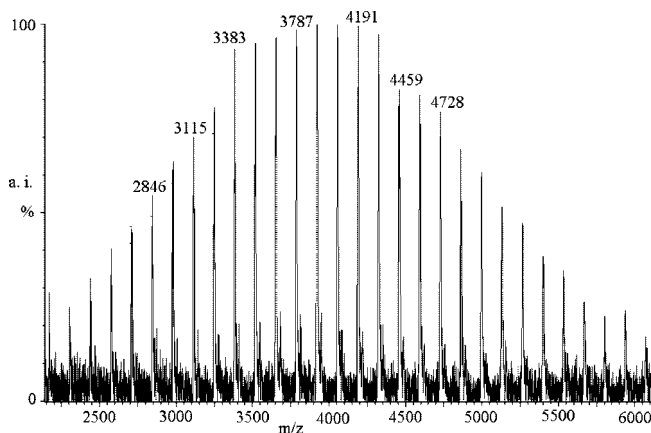


Figure 12. MALDI-TOF spectrum of POMESt-ClSt-Br prepared using [*p*MeOStCl] = 0.001 mol L^{-1} , [DTBP] = 0.006 mol L^{-1} , [*SnBr}_4*] = 0.009 mol L^{-1} , and $\text{CH}_2\text{Cl}_2/\text{MeCHx}$ (50/50, v/v) at $-40\text{ }^\circ\text{C}$.

in the presence of *p*ClSt at $-40\text{ }^\circ\text{C}$ are shown in Figure 13. The conversion as well as number-average molecular weight reached a limiting value in 30 min. The M_n of the polymer, determined by GPC, was in reasonable agreement with the theoretical one. The polydispersity index of the polymers was in the range of 1.3–2.1. ^1H NMR spectra of these polymers show the absence of methoxy chain end protons at $\sim 3\text{ ppm}$ due to complete capping. The limiting conversions, molecular weights, and k_p/k_{12} values are shown in Table 11. The average reactivity ratio decreases from 670 at $-40\text{ }^\circ\text{C}$ to 454 at $0\text{ }^\circ\text{C}$.

From the Arrhenius plot (Figure S22 in Supporting Information) $E_p - E_{12} = -6.4\text{ kJ mol}^{-1}$ was determined.

Figure S23 shows the time vs conversion plots for the competition experiment carried out in $\text{CH}_2\text{Cl}_2/\text{MeCHx}$, (50/50, v/v) at $-40\text{ }^\circ\text{C}$. (See Tables S23 and S24 in Supporting Information for the results at -20 and $0\text{ }^\circ\text{C}$.) The limiting conversions, molecular weights, and k_p/k_{12} values are shown in Table 12.

From the Arrhenius plot (see Figure S24 in Supporting Information) $E_p - E_{12} = -6.3\text{ kJ mol}^{-1}$ was calculated.

Comparison of Reactivity Ratios with Published Values. The reactivity ratios determined in this paper could be compared to published reactivity ratios calculated from copolymerization experiments. Unfortunately, a comprehensive reexamination of several hundred published values found only a small number of reliable reactivity ratios.¹⁹ Reactivity ratios of *p*MeOSt in the copolymerization of *p*MeOSt with *p*MeSt initiated by iodine at $0\text{ }^\circ\text{C}$ have been reported by Yamamoto and Higashimura.²⁰ In CCl_4 , $\text{CH}_2\text{Cl}_2/\text{CCl}_4$ (2/1), or CH_2Cl_2 in the presence of the common ion salt $n\text{-Bu}_4\text{NI}_3$ reactivity ratios varied between ~ 26 and 29 , which are similar to our values in Table 8. In CH_2Cl_2 in the absence of the common ion salt, however, $r_{p\text{MeOSt}} = 11$ was reported, which would be difficult to explain since recent studies indicated similar reactivity of

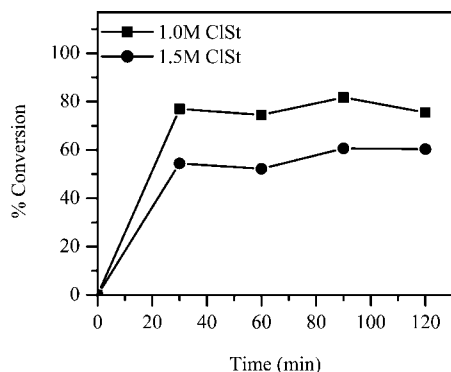


Figure 13. Time vs conversion plots from the competition experiments between *p*MeOSt and *p*ClSt in CH_2Cl_2 at -40°C . [*p*MeOSt] = 0.2 mol L^{-1} ; [*p*MeOStCl] = 0.002 mol L^{-1} ; [DTBP] = 0.006 mol L^{-1} ; [*p*ClSt] = 1.0 and 1.5 mol L^{-1} .

Table 11. Limiting Conversion, Molecular Weight, and k_p/k_{12} Values in the Competition Reactions between *p*MeOSt and *p*ClSt in CH_2Cl_2 at Different Temperatures^a

<i>p</i> ClSt (mol L^{-1})	temp ($^\circ\text{C}$)	conv (%)	M_n (GPC)	PDI	k_p/k_{12} (conv)	k_p/k_{12} (DP _∞)	k_p/k_{12} (av)
1.0	-40	75.5	9100	1.5	702	566	634
1.5	-40	60.3	8300	1.3	686	721	703
1.0	-20	69.1	10200	1.7	586	713	649
1.5	-20	49.9	7200	2.2	518	576	547
1.0	0	55.9	8900	1.8	409	543	476
1.5	0	39.7	6400	2.0	379	485	432

^a [*p*MeOSt] = 0.2 mol L^{-1} ; [*p*MeOStCl] = 0.002 mol L^{-1} ; [DTBP] = 0.006 mol L^{-1} ; [*p*ClSt] = 1.0 and 1.5 mol L^{-1} .

Table 12. Limiting Conversion, Molecular Weight, and k_p/k_{12} Values in the Competition Reactions between *p*MeOSt and *p*ClSt in $\text{CH}_2\text{Cl}_2/\text{MeCHx}$ (50/50, v/v) at Different Temperatures^a

<i>p</i> ClSt (mol L^{-1})	temp ($^\circ\text{C}$)	conv (%)	M_n (GPC)	PDI	k_p/k_{12} (conv)	k_p/k_{12} (DP _∞)	k_p/k_{12} (av)
0.5	-40	52.2	21 000	1.47	804	762	783
0.75	-40	33.5	17 000	2.01	768	752	760
0.5	-20	72.0	19 000	1.47	636	615	625
0.75	-20	55.9	15 800	1.61	614	666	640
0.5	0	60.1	16 800	1.34	459	491	475
0.75	0	44.2	13 200	1.39	437	507	472

^a [*p*MeOSt] = 0.2 mol L^{-1} ; [*p*MeOStCl] = 0.001 mol L^{-1} ; [DTBP] = 0.006 mol L^{-1} ; [*p*ClSt] = 0.009 mol L^{-1} , time = 120 min.

Table 13. Relative Reactivities ($1/r$)/10⁻² of Monomers toward the *Pp*MeOSt⁺ Cation at -40 and 0°C

monomer	CH_2Cl_2 $-40/0^\circ\text{C}$	$\text{CH}_2\text{Cl}_2/\text{MeCHx}$ $-40/0^\circ\text{C}$
<i>p</i> MeSt	2.43/3.33	2.38/3.57
IB	0.50/0.58	0.37/0.59
St	0.29/0.50	0.34/0.51
<i>p</i> ClSt	0.15/0.22	0.13/0.21

free ions and ion pairs. Higashimura and co-workers also reported $r_{p\text{MeOSt}} = 22.8$ in the copolymerization of *p*MeOSt with St in benzene at 30°C ,²¹ which is much lower than the value we report in this paper. Toppare et al. also studied the cationic copolymerization of *p*MeOSt with St in 1,2-dichloroethane at

30°C ²² and calculated $r_{p\text{MeOSt}} = 0.8\text{--}1.6$; however, this value seems completely unacceptable.

Comparison of Monomer Reactivities Based on k_p/k_{12} Values with Nucleophilicity Parameters. The above results may be compared with the nucleophilicity (*N*) parameters $N_{p\text{MeOSt}} \approx 3.31$ (approximate number), $N_{p\text{MeSt}} = 1.70$, $N_{\text{IB}} = 1.11$, $N_{\text{St}} = 0.78$, and $N_{p\text{ClSt}} \approx 0.21$ (approximate number) reported by Mayr.²³ According to these values at 20°C , *p*MeOSt is 41, 160, 340, and 1240 times more reactive than *p*MeSt, IB, St, and *p*ClSt, respectively. To compare our results from the competition reactions, the k_p/k_{12} was extrapolated to 20°C using the activation energy values from the Arrhenius plots (Figures S9, S14, S19, and S24 in Supporting Information). According to these values, *p*MeOSt is 24, 140, 170, and 400 times more reactive than *p*MeSt, IB, St, and *p*ClSt, respectively, in $\text{CH}_2\text{Cl}_2/\text{MeCHx}$ (50/50, v/v). These values follow the same trend as the *N* values.

Comparison of Monomer and Cation Reactivity. The inverse reactivity ratio, which gives the ratio of the rate constant of the reaction of a propagating center with another monomer to that of its own monomer, is often used to characterize monomer reactivities. Table 13 lists the $1/r$ values calculated for -40°C . Independent of the solvent polarity and temperature the order of monomer reactivity is *p*MeOSt > *p*MeSt > IB > St > *p*ClSt, which is in accord with theoretical considerations and published nucleophilicity parameters.

Using the reactivity ratios and the propagation rate constants (k_p), the cross-propagation rate constant (k_{12}) values were calculated (Table 14).

In Table 14 any vertical column gives the order of monomer reactivities. The data in any horizontal row provide the cation reactivities against a standard monomer. Although the data are rather limited at present, a few observations can be made. For instance, the *Pp*MeOSt⁺ cation is about 10⁶ times less reactive compared to the *Pp*MeSt⁺ cation. Interestingly, replacing the *p*-methyl substituent in *p*MeSt with the *p*-methoxy group increases the reactivity of monomer by only a factor of 42. Similarly, the *Pp*MeOSt⁺ cation is about 2×10^7 times less reactive compared to the *PSt*⁺ cation; however, *p*MeOSt is only 300 times more reactive than St. The electrophilicity of cations is inversely related to the nucleophilicity of the parent monomers. However, the long-held view¹⁰ that these effects cancel each other is inaccurate as the substituent has a much larger effect on the cation reactivity than on the monomer reactivity. This trend is similar to that observed in radical polymerization. Research is in progress to complete Table 14 and extend it to include other monomers.

Conclusions

Carbocation–olefin reactions that terminate after a single addition to yield the [1:1] adduct are highly useful to determine reactivity ratios from which monomer structure–reactivity scales can be constructed. With the known propagation rate constants the cross-propagation rate constants could be calculated. On the basis of these values, structure–reactivity scales for monomers and carbocations could be established. According to these

Table 14. Rate Constants (L mol⁻¹ s⁻¹) for Cation–Monomer Reactions in $\text{CH}_2\text{Cl}_2/\text{MeCHx}$ (50/50, v/v) at -40°C

monomer	polymer cation				
	<i>Pp</i> MeOSt ⁺	<i>Pp</i> MeSt ⁺	PIB ⁺	<i>PSt</i> ⁺	<i>Pp</i> ClSt ⁺
<i>p</i> MeOSt	7800	diffusion limited	diffusion limited	diffusion limited	diffusion limited
<i>p</i> MeSt	186	2×10^8 ^a	diffusion limited	diffusion limited	diffusion limited
IB	29		7×10^8	diffusion limited	diffusion limited
St	26			4×10^9	diffusion limited
<i>p</i> ClSt	10				3×10^9

^a Estimated value from $k_p = 1 \times 10^9$ L mol⁻¹ s⁻¹ in CH_2Cl_2 .

results, the effect of substituents on carbocation reactivity is much larger than their effect on monomer reactivity.

Acknowledgment. Financial support by the National Science Foundation (CHE-0548466) is gratefully acknowledged. N.K. thanks Dr. P. De and Prof. S. Keki for various suggestions.

Supporting Information Available: Arrhenius plots of reactivity ratios, ^1H NMR spectra of capped polymers, and detailed results of competition experiments for M_n , PDI, and limiting conversion in CH_2Cl_2 and $\text{CH}_2\text{Cl}_2/\text{MeCH}_3$ at -40 , -20 , and 0 °C. This material is available free of charge via the Internet at <http://pubs.acs.org>.

References and Notes

- (1) De, P.; Faust, R. Carbocationic Polymerization. In *Macromolecular Engineering. Precise Synthesis, Materials Properties, Applications*; Matyjaszewski, K., Gnanou, Y., Leibler, L., Eds.; Wiley: Weinheim; 2007; Vol. 1, pp 57–101.
- (2) Mayr, H. In *Cationic Polymerization: Mechanisms, Synthesis and Applications*; Matyjaszewski, K., Ed.; Marcel Dekker: New York, 1996; pp 51–136.
- (3) Sipos, L.; De, P.; Faust, R. *Macromolecules* **2003**, *36*, 8282–8290.
- (4) De, P.; Faust, R.; Schimmel, H.; Ofial, A. R.; Mayr, H. *Macromolecules* **2004**, *37*, 4422–4433.
- (5) De, P.; Faust, R. *Macromolecules* **2004**, *37*, 7930–7937.
- (6) De, P.; Sipos, L.; Faust, R.; Moreau, M.; Charleux, B.; Vairon, J.-P. *Macromolecules* **2005**, *38*, 41–46.
- (7) De, P.; Faust, R. *Macromolecules* **2004**, *37*, 9290–9294.
- (8) De, P.; Faust, R. *Macromolecules* **2005**, *38*, 5498–5505.
- (9) Roth, M.; Mayr, H. *Macromolecules* **1996**, *29*, 6104–6109.
- (10) Matyjaszewski, K.; Pugh, C. In *Cationic Polymerization: Mechanisms, Synthesis and Applications*; Matyjaszewski, K., Ed.; Marcel Dekker: New York, **1996**; pp 137–264.
- (11) Mayr, H.; Ofial, A. R.; Schimmel, H. *Macromolecules* **2005**, *38*, 33–40.
- (12) (a) Mayr, H.; Bug, T.; Gotta, M. F.; Hering, N.; Irrgang, B.; Janker, B.; Kempf, B.; Loos, R.; Ofial, A. R.; Remennikov, G.; Schimmel, H. *J. Am. Chem. Soc.* **2001**, *123*, 9500–9512. (b) Mayr, H. *Angew. Chem., Int. Ed.* **1990**, *29*, 1371–1384. (c) Mayr, H.; Kempf, B.; Ofial, A. R. *Acc. Chem. Res.* **2003**, *36*, 66–77.
- (13) Bae, Y. C.; Hadjikyriacou, S.; Schlaad, H.; Faust, R. *NATO Sci. Ser. E: Appl. Sci.* **1999**, *359*, 61.
- (14) De, P.; Faust, R. *Macromolecules* **2006**, *39*, 6861–6870.
- (15) De, P.; Faust, R.; Schimmel, H.; Ofial, A. R.; Mayr, H. *Macromolecules* **2004**, *37*, 4422–4433.
- (16) Schlaad, H.; Kwon, Y.; Sipos, L.; Faust, R.; Charleux, B. *Macromolecules* **2000**, *33*, 8225–8232.
- (17) (a) Moreau, M.; Matyjaszewski, K.; Sigwalt, P. *Macromolecules* **1987**, *20*, 1456–1464. (b) Sawamoto, M.; Higashimura, T. *Macromolecules* **1979**, *12*, 581–585.
- (18) (a) Nonaka, H.; Ouchi, M.; Kamigaito, M.; Sawamoto, M. *Macromolecules* **2001**, *34*, 2083–2088. (b) Nonaka, H.; Kamigaito, M.; Sawamoto, M. *Polym. Prepr. Jpn.* **1999**, *48*, 1125.
- (19) (a) Kennedy, J. P.; Kelen, T.; Tudos, F. *J. Polym. Sci.* **1975**, *13*, 2277–2289. (b) Kelen, T.; Tudos, F.; Turcsanyi, B.; Kennedy, J. P. *J. Polym. Sci.* **1977**, *15*, 3047–3074.
- (20) Yamamoto, K.; Higashimura, T. *J. Polym. Sci.* **1976**, *14*, 2621–2629.
- (21) Hasegawa, K.; Masuda, T.; Higashimura, T. *Macromolecules* **1975**, *8*, 255–259.
- (22) Toppare, L.; Eren, S.; Ozel, O.; Akbulut, U. *J. Macromol. Sci., Chem.* **1984**, *A21*, 1281–1286.
- (23) (a) Mayr, H. In *Ionic Polymerizations and Related Processes*; Puskas, J. E., Michel, A., Barghi, S., Paulo, C., Eds.; NATO Sci. Ser. E: Applied Sciences; Kluwer Academic Publishers: Dordrecht, 1999; Vol. 359, pp 99–115. (b) Mayr, H.; Kempf, B.; Ofial, A. R. *Acc. Chem. Res.* **2003**, *36*, 66–77. (c) Sigwalt, P.; Moreau, M. *Prog. Polym. Sci.* **2006**, *31*, 44–120.

MA800120H